Biogenic Si analysis in volcanically imprinted lacustrine systems : the case of Lake Rutundu (Mt. Kenya)

Reference:

Barão Lúcia, De Cort Gijs, Meire Patrick, Verschuren Dirk, Struyf Eric.- Biogenic Si analysis in volcanically imprinted lacustrine systems : the case of Lake Rutundu (Mt. Kenya)
Biogeochemistry - ISSN 0168-2563 - 125:2(2015), p. 243-259
DOI: http://dx.doi.org/doi:10.1007/s10533-015-0125-0

Biogenic Si analysis in volcanically imprinted lacustrine systems: the case of Lake Rutundu (Mt. Kenya)

Lúcia Barão . Gijs De Cort . Patrick Meire .Dirk Verschuren . Eric Struyf

Abstract Diatoms are important primary producers in lake ecosystems and, as a sink for dissolved (DSi) and biogenic silica (BSi) originating from land, can significantly impact the global Si cycle. After burial in lake sediments, resistant diatom frustules can also be used for reconstructions of past ecosystem change. The BSi content of lake sediments is thus often used as a proxy for past diatom productivity, and measured using a time-step analysis of Si extracted in 0.1 M Na_2CO_3. However, studies in soils and ocean sediments have shown that also certain non-biogenic Si fractions are prone to dissolve in alkaline solutions, contributing to a potential overestimate of sedimentary BSi concentration. In lakes, volcanic and terrestrial Si compounds reactive at high pH are likely to interfere with the analysis. In this study we used a continuous analysis of Si and Al extracted in 0.5 M NaOH and a new mathematical model improved from Koning et al. (Aquat Geochem 8:37–67, 2002) to distinguish between biogenic and non-biogenic Si fractions in lake-sediment extracts. We tested this approach in 43 samples of a 19,000-year sediment sequence recovered from Lake Rutundu, a volcanic crater lake on Mt. Kenya. Our results show that a significant fraction of the extractable Si is of non-biogenic origin, especially in the part of the sequence deposited during the glacial period. We conclude that this technique is essential for the characterization of different Si phases, and in particular the diatom-derived BSi, in the sediment of lakes situated in volcanic catchments. It allows calculating a correction, based on the distinct Si:Al ratio of each of those Si phases, that eliminates the contribution from non-BSi fractions.

Keywords Lakes - Diatoms - Volcanic interference- Alkaline extractions - Continuous analysis

Introduction

Dissolved silica (DSi), produced by the weathering of silicate minerals, is transported to coastal zones and the oceans through river systems (e.g. Street-perrott and Barker 2008; Cornelis et al. 2011; Tréguer and De La Rocha 2013). In many aquatic environments, DSi is to a large part incorporated into diatom frustules as biogenic silica (BSi) (e.g. Ragueneau et al. 2006). This is most apparent in the ocean: here diatoms can drive

DSi concentrations down to values limiting their own growth, and rapid BSi recycling occurs upon diatom die-off. Only about 3 % of the BSi eventually becomes deposited in ocean sediments (Tréguer and De La Rocha 2013), a percentage which is to a large part replenished from land through riverine DSi. In recent decades, major attention has been directed towards this DSi flux from land to ocean. Advances in understanding of the terrestrial Si biogeochemical cycle show that terrestrial ecosystems act as a filter (Conley 2002; Struyf and Conley 2012) between Si weathering and riverine Si transport, and that DSi input to coastal waters and oceans is highly dependent on processes taking place in the soil (Laruelle et al. 2009; Struyf et al. 2010; Carey and Fulweiler 2012) and at the catchment scale (Humborg et al. 2000; Hartmann et al. 2009).

Lakes and man-made reservoirs play an important role in the global Si budget, since they represent a (temporary) sink for a significant part of the weathered DSi that has passed through the terrestrial ecosystem filter. Conley et al. (2000) found that concentrations of riverine DSi are inversely related to the percent area of a catchment occupied by lakes or reservoirs. Recently, Frings et al. (2014) estimated that the BSi trapped in lakes equates to 21–27 % of the total DSi delivered to oceans.

Diatoms preserved in the sedimentary record of lakes have often been used as indicators (proxies) for reconstructing past ecosystem changes, on account of their short generation times and sensitivity to a diverse range of biologically relevant environmental variables (Stoermer and Smol 1999; Battarbee et al. 2001). Besides proxies based on changes in species assemblages through time (Smol and Cumming 2000) or the stableisotopic signature of oxygen and carbon contained in diatom frustules (Leng and Barker 2006; Barker et al. 2013), the percent concentration of BSi measured in lake sediments is often used as a proxy for past diatom productivity (Conley and Schelske 2001),which in turn can be linked to climate variability (e.g. Johnson et al. 2001) or the impact of human activity on ecosystem health (e.g. Verschuren et al. 2002; Theissen et al. 2012). As such, sedimentary BSi content contains unique information about the spatial and temporal distribution of diatom primary production both in the ocean (Broecker 1994;

Ragueneau et al. 2000) and in lakes, from arctic (e.g. Finkelstein and Gajewski 2007) and temperate (e.g. Schelske et al. 1983) to (sub-)tropical regions (e.g., Johnson et al. 2002; Felton et al. 2007).
The method most often used to measure BSi in sediments is a time-step analysis of Si extracted using Na_2CO_3 as solvent (DeMaster 1981; Mortlock and Froelich 1989). Samples are digested for 5 h at 85 _C; the higher solubility of diatoms compared to silicate minerals allows to correct for any mineral dissolution using a linear regression of the Si concentrations extracted after 3, 4 and 5 h. Although this protocol has been extensively used for marine sediments, Koning et al. (2002) showed that clay minerals can also react in alkaline solutions. This results in over-estimation of the BSi content, especially in cases where heavy loading of clastic mineral sediment blurs a relatively modest diatom-derived signature. Koning et al. (2002) reached their conclusion thanks to a continuous analysis of Si and Al during the extraction, since the changing ratio between Si and Al (Si:Al) can help reveal the presence of clay minerals (Kamatani and Oku 2000; Ragueneau et al. 2005). Lately it is acknowledged that also other fractions of Si, resulting from pedogenic processes in soils containing significant amounts of Al, may be extracted together with diatoms and phytoliths, further compromising correct determination of true BSi in soils and sediments (Cornelis et al. 2014; Bara□b et al. 2014). Also source rocks of volcanic origin can potentially cause contamination, since alkaline solvents readily dissolve the amorphous Si glass found in tephra deposits and volcanic soils (Clymans et al. 2014).
The specific identification of these various Si phases in lake sediments and their influence on the validity of BSi as palaeo-environmental indicator remain poorly studied. However, it is clear that their contribution to the total pool of alkaline-extractable Si (AlkExSi) may be significant. Here we address the issue by using continuous analyses of Si and Al and a mathematical model improved from Koning et al. (2002) to distinguish between biogenic (presumably diatom-derived) Si and non-biogenic ('contaminating') Si phases in a 19,000-year sediment sequence from Lake Rutundu, a small volcanic crater lake on Mt. Kenya (East Africa). The choice of Lake Rutundu for this case study is fitting, since this site has been the subject of intensive palaeo-environmental research (Barker et al. 2000; Ficken et al. 2002; Wooller et al. 2003; Street-Perrott et al. 2004, 2007, 2008) and the use of alkaline extraction methods for determining its sedimentary BSi content was flagged as problematic (Street-Perrott et al. 2008). Using parallel extractions on a subset of samples, we compared results of our continuous analysis to those of a time-step analysis following DeMaster (1981), and assessed the codissolution of Al in 0.5 MNa_2CO_3 to identify whether contaminant fractions also compromise BSi determination in a weaker base environment. Our results show that continuous paired Si and Al analysis is important to correctly determine BSi content in the sediments of Lake Rutundu, and by extension all lakes situated in volcanic catchments.

Materials and methods

Lake Rutundu sediments

This study is based on sediment core Rut09-1P collected in August 2009 from the deepest point (11 m) of Lake Rutundu (0º02'30″N, 37º 27'50″E), a 10-ha volcanic crater lake situated at 3080 m elevation on the northeastern flank of Mount Kenya. Outflow occurs underground through porous volcanic layers, and lake waters are thus fresh and dilute, with a conductivity of 35 lS cm^{-1} and a circum-neutral pH of 7.6. The dissolved-Si concentration of surface water at the time of coring was very low (\0.1 mg L^{-1}). Situated in equatorial East Africa, the local climate is characterized by a bimodal seasonal rainfall pattern caused by the twice-yearly passage of the intertropical convergence zone (ITCZ), with long (March– May) and short (October–November) rainy seasons of 100–200 mm m^{-1} alternating with two drier seasons when precipitation is low but still at least 20 mm/month. Lake Rutundu is situated just above the present-day tree-line, where mean annual temperature is about 10 ºC with occasional night-time freezing. As is typical for tropical mountains, seasonal variability in temperature is low (ca. 2 ºC), but the day-night contrast is high (on the order of 14ºC).
Several overlapping core sections were collected using gravity and piston-coring techniques, which were combined into a single composite sequence comprising 324 cm of lacustrine sediment accumulation, interrupted by a tephra layer of volcanic glass at 248–249 cm (Fig. 1a). Also two sandy turbidites were identified at 254 256.5 and 312–314 cm depth. Sediment water and organic-matter content were determined by drying overnight at 105 _C, followed by burning at 550 _C according to the loss-on-ignition technique (Dean 1974). The sediment chronology is based on 19 accelerator-mass-spectrometry (AMS) radiocarbon (^{14}C) dates supplemented by ^{210}Pb dating of the recent deposits. The construction of this age model will be described in detail elsewhere (De Cort et al. in preparation); for this study it only serves to distinguish between full-glacial, late-glacial and Holocene sediments showing different patterns of Si

dissolution. Variation in the diatom productivity of Lake Rutundu over this time was previously estimated on the basis of frustule-volume ('biovolume') calculations applied to fossil diatom assemblages identified at the species or genus level (Barker et al. 2000).

BSi determination using continuous analysis of an extraction in 0.5 M NaOH

The continuous analysis technique (Koning et al. 2002;Barão et al. 2014) traces the dissolution of Si and Al in real time at 15-s intervals. In total, 43 freeze-dried sediment samples (10–26 mg) from along the Rutundu sequence were mixed with 0.5 M NaOH in a stainless steel vessel that was itself submerged in a water bath at 85 ºC. A rotor ensured consistent contact between solid and solution. The vessel was connected to an autoanalyser which continuously measured dissolved Si (Grasshoff et al. 1983) and Al content (Hydes and Liss 1976). The dissolution curves of both Si and Al were used to estimate the sediment's BSi content. In this procedure, we initially distinguished two main phases: (1) the non-linear phase, when all Si with high solubility is digested; and (2) the linear phase, when any silicate minerals with low solubility continue to dissolve. Manifestation of the linear phase requires a sufficiently long duration of the alkaline extraction (Barão et al. 2015). The non linearly extracted fraction (i.e., the Si concentration obtained after correction for simultaneous slow dissolution of mineral Si) is here defined as 'alkaline-extractable Si' or $AlkExSi_{NaOH}$, accounting for the fact that it often includes fractions other than biogenic (Koning et al. 2002). To identify the origin of those fractions,we fitted the non-linear portion of the dissolution curve to a first-order model (with n possible fractions) while the linear portion is fitted to a linear model with one fraction (Eq. 1). The model best fitting the measured Si and Al dissolution curves was chosen based on F tests, and this determined the number of AlkExSi fractions coexisting in the sample (Barão et al. 2015). Each of these fractions is characterized by a specific Si:Al ratio and reactivity (k). AlkExSi fractions accounting for less than 1 % of the total AlkExSi pool were not considered.

$$\begin{aligned} Si_t &= \left(\sum_{i=1}^{n} AlkExSi_i \times \left(1 - e^{-k_i \times t}\right)\right) + b \times t \\ Al_t &= \left(\sum_{i=1}^{n} \frac{AlkExSi_i}{Si:Al_i} \times \left(1 - e^{-k_i \times t}\right)\right) \\ &\quad + \frac{b \times t}{Si:Al_{min}} \end{aligned} \qquad (1)$$

Si_t is the Si dissolved at time t, $AlkExSi_i$ is fraction i of the Si extracted in NaOH, k_i is the reactivity of fraction i, b is the regression slope of the mineral dissolution, Al_t is the Al dissolved at time t, $Si:Al_i$ is the Si:Al ratio of fraction i, $Si:Al_{min}$ is the Si/Al ratio of the mineral fraction and n is the number of fractions.

The Si:Al ratios of the different fractions dissolving in NaOH can be used to evaluate their origin. Si:Al ratios higher than five are assumed to be of biogenic origin, since diatoms and phytoliths do not accumulate excessive amounts of Al (van Bennekom et al. 1989; Ren et al. 2013). Higher Al contents are compatible with e.g. reactive clay minerals or weathered products resulting from soil formation and volcanic processes (Clymans et al. 2014; Barão et al. 2014).

BSi determination using time-step analysis of an extraction in 0.1 M Na_2CO_3

A subset of 10 representative core samples were also extracted in 0.1 M Na_2CO_3 using a modified DeMaster (1981) method. These samples were mixed in plastic vessels with 180 mL of the solvent and submerged in a stirred water bath at 85 _C. Their weight was identical as in the continuous analysis, to ensure comparable conditions. One mL of solution was taken after 5, 13, 19, 25, 30, 36, 70, 105, 140, 205, 270 and 330 min, and analysed for dissolved Si and Al in the auto-analyser. Results from the last three time steps (205, 270 and 330 min) were used to estimate the rate of (slow) mineral dissolution. The zero-time intercept of the extrapolated regression slope of the dissolved Si measured at these three time steps is normally assumed to represent BSi (DeMaster 1981). Since we do not assume a priori that all Si dissolving non-linearly is of biogenic origin, we identify this zero-time concentration of extractable Si as $AlkExSi_{Na2CO3}$. Although the method used for calculating $AlkExSi_{Na2CO3}$ is similar to that of DeMaster (1981), measuring Si and Al concentrations at several additional time steps at the start of the experiment allowed better comparison with the results of our continuous analysis ($AlkExSi_{NaOH}$) regarding the initial dissolution patterns and co-dissolution of Al enriched fractions.

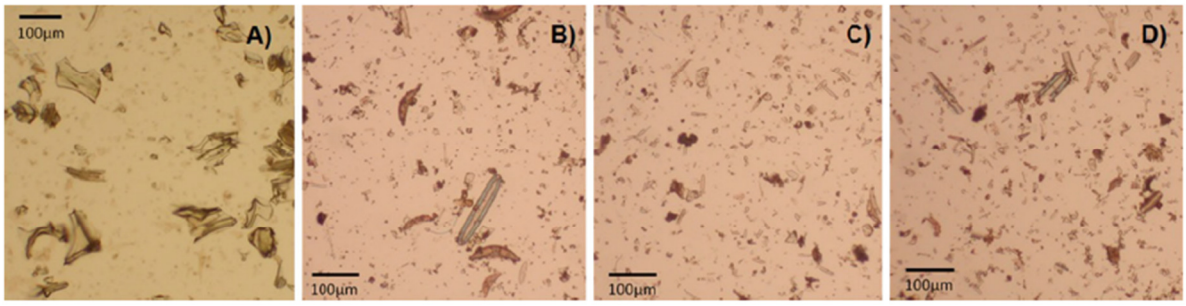

Fig. 1 Smear-slide images of the late-glacial tephra layer (at 248–249 cm depth) dominated by amorphous volcanic glass (a), and of representative diatom-containing lacustrine sediments in Lake Rutundu dated to the late glacial period (b), the early Holocene (c) and the mid Holocene (d)

Results and discussion

Variation in Si dissolution curves

Most Si dissolution curves from Lake Rutundu sediments showed a very specific pattern comprised of two distinct stages: a slow start followed by strong acceleration of Si dissolution within the first few minutes, followed by a decrease in the dissolution rate. This sigmoidal dissolution pattern varied across samples and was almost absent in the lower portion of the core (below 230 cm, i.e. the glacial and late-glacial parts of the sequence) where Si dissolution followed a simple negative exponential curve before reaching the linear phase (Fig. 2). Al dissolution, in contrast, consistently followed a negative exponential curve throughout the sequence. Consequently, first-order non-linear model equations did not fit well to our data and could not be used. This dissolution pattern has not previously been reported in studies where this same technique was used, either on marine sediments (Koning et al. 2001; Raimonet et al. 2014) or soils (Saccone et al. 2007; Barão et al. 2014). We therefore developed a new set of mathematical equations to fit Si and Al dissolution data from Lake Rutundu, hypothesizing that the sigmoidal dissolution pattern of Si is due to simultaneous dissolution of biogenic and non-biogenic fractions.
Saccone et al. (2007) observed a similar sigmoidal pattern when dissolving pure phytoliths in NaOH. This largely comprised of volcanic glass with a minor mineral fraction and complete absence of diatoms (Fig. 1a). The Si dissolution curve from this tephra layer shows no sigmoidal pattern (Fig. 3b), confirming that the latter is distinctive for diatom dissolution. The observed negative-exponential dissolution curve is consistent with the dissolved material being derived from volcanic rocks (Clymans et al. 2014). Based on this evidence, our mathematical equations assume that the observed AlkExSi concentrations are the sum of a biogenic fraction characterized by a sigmoidal increase (Eq. 2), and of one or more nonbiogenic fractions characterized by a negative exponential increase (Eq. 1) and variable Si:Al ratios.

$$Si_t = \frac{AlkExSi_1 \times N_0}{N_0 + (AlkExSi - N_0) \times e^{k_1 . t}}$$
$$Al_t = \frac{AlkExSi_1 \times N_0}{N_0 + (AlkExSi - N_0) \times e^{k_1 . t}} \times \frac{1}{Si/Al_1} \quad (2)$$

$AlkExSi_1$ is the alkaline extracted Si corresponding to the fraction calculated with Eq. 1, while k_1 and $Si:Al_1$ represent its reactivity and Al content. The N_0 parameter corresponds to the initial delay time of the curve. The totality of the Si and Al dissolution curves in any sample containing both fractions can then be represented by a combination of Eqs. 1 and 2 (Eq. 3).

$$Si_t = \frac{AlkExSi_1 \times N_0}{N_0 + (AlkExSi - N_0) \times e^{k_1 . t}} + \sum_{i=2}^{4} AlkExSi_i \times \left(1 - e^{-k_i . t}\right) + b.t$$
$$Al_t = \left(\frac{AlkExSi_1 \times N_0}{N_0 + (AlkExSi - N_0) \times e^{k_1 . t}}\right) \times \frac{1}{Si/Al_1} + \sum_{i=2}^{4} \frac{AlkExSi_i}{Si/Al_i} \times \left(1 - e^{-k_i . t}\right) + \frac{b.t}{Si/Al_{\min}} \quad (3)$$

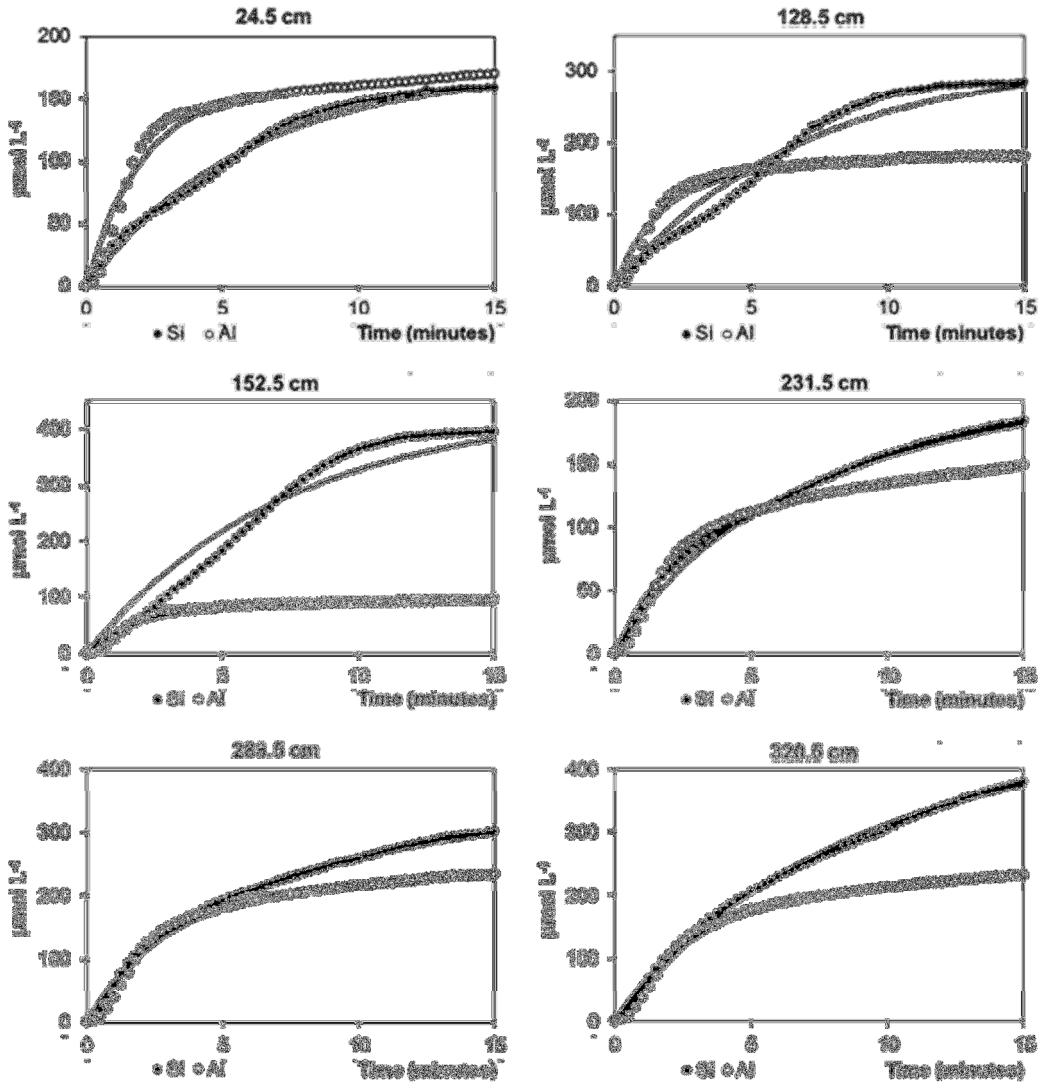

Fig. 2 Dissolution curves of Si (black circles) and Al (white circles; both in lmol L^{-1}) in the first 15 min of continuous analysis of AlkExSi in six representative samples (identified by their mid-depth value) from the Lake Rutundu sediment record. The full black lines represent the best-fitting first-order nonlinear models. Note the variable scale of the ordinate axis

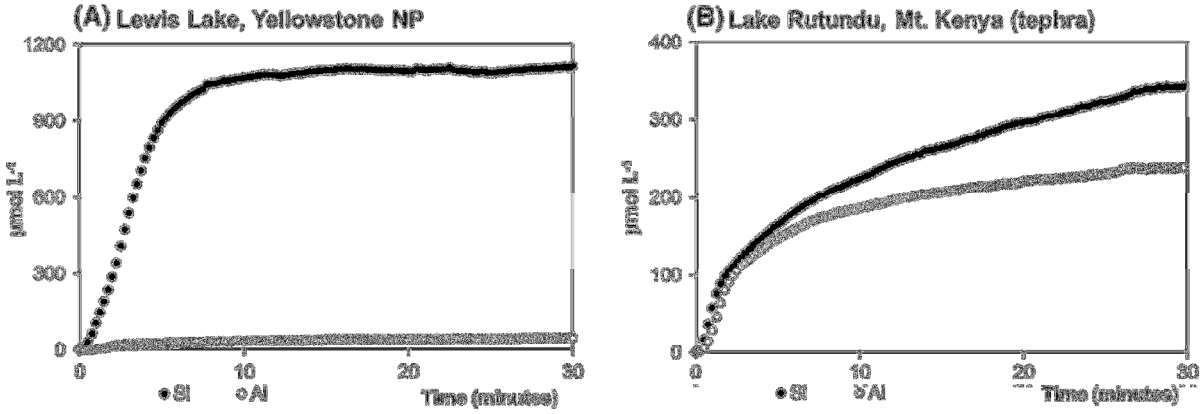

Fig. 3 Dissolution curve of Si in sediment samples from Lewis Lake in Yellowstone National Park (a) (Barão et al. 2015) and from the Lake Rutundu tephra sample at 248–249 cm (b). Note the different scale on the ordinate axis

To test our hypothesis mathematically, we compared the results of the traditional model-fitting approach (Eq. 1) with those of the new approach (Eq. 3). F tests confirmed that the new approach resulted in a

better model fit for all analyzed samples except the tephra layer (248–249 cm), confirming that in a sample with no trace of diatoms, the sigmoidal signal is absent.

Determining biogenic Si in Lake Rutundu sediments using the continuous analysis

Biogenic Si fractions in the AlkExSi pool that show a sigmoidal dissolution pattern were thus successfully separated from non-biogenic 'contaminant' fractions. In the large majority of cases, the biogenic fractions displayed very high Si:Al ratios (_1000), confirming their biogenic origin (Koning et al. 2002). Only one sample showed a low Si:Al ratio of 3 (231–232 cm, Table 1) for the biogenic fraction, showing remaining difficulty of our current model to isolate BSi in this local case. True BSi was consistently lower than total $AlkExSi_{NaOH}$, indicating that other alkaline-reactive but non-biogenic Si fractions are present in all Lake Rutundu samples and thatNaOHis able to extract them. Common Si contributors such as quartz, however, are poorly reactive in alkaline solutions and thus expected to dissolve linearly with time during the experiment. The percent contribution of these contaminant fractions increases with depth in the Rutundu sequence, especially in its pre-Holocene section (220–320 cm) where non-biogenic reactive Si represents on average
4.9 % (range 3.2–7.1 %) of total dry sediment mass; in the Holocene section it contributes on average 2.4 % (range 0.8–6.7 %; Fig. 4). Given the relatively modest concentrations of total $AlkExSi_{NaOH}$ (1.7–9.8 %; mean 5.3 %) and thus also of true BSi (0.0–8.0 %, mean 2.1 %) in these lake sediments, the contaminants' presence strongly biases the estimation of BSi.

Origin and significance of non-biogenic Si in Lake Rutundu sediments

Our continuous extraction analysis identified several Si fractions other than biogenic Si (Table 1; Fig. 5). All these fractions dissolve according to a negative exponential pattern covered by a first-order non-linear model, clearly distinct from the sigmoidal pattern of biogenic Si. These contaminants (from the perspective of BSi determination) can be distinguished from each other on the basis of their Si:Al ratios and their reactivity. Two main contributors to AlkExSi were identified: one with high Si:Al ratios (11–1250) and low reactivity (average 0.21 min^{-1}) and another with much lower Si:Al ratios (\1) and higher reactivity (average 0.73 min^{-1}) (Fig. 5). A third type of contamination is present only in four Rutundu samples between 216–217 and 256–257 cm depth, and seems to relate to the local occurrence of minerals with Si:Al ratios ranging between 1 and 5 (Koning et al. 2002), i.e. slightly more reactive than the abundant nonreactive silicate minerals (Table 1). The imprint of minerals is normally reflected in parameter b, i.e. the regression slope of the rate of linear dissolution against time. Exceptionally in these four samples, minerals also contributed to AlkExSi, suggesting a lower degree of crystallinity and a consequent higher reactivity in the alkaline solvent. At this time we must refrain from speculating further on their origin, except that the presence of such compounds suggests that broadly during the late-glacial period, some Rutundu catchment minerals experienced an intermediate degree of weathering. The non-biogenic AlkExSi fraction with high Si:Al ratios is identified as volcanic glass, based on mathematical similarity of its dissolution trajectory with that of the tephra sample (compare Fig. 5 with Fig. 3). The second contaminant fraction is enriched in aluminium (Si:Al\1), so a volcanic glass origin can be ruled out (Cornelis et al. 2014). Since the majority of Si:Al ratios for this fraction are lower than 1 we hypothesize that these sediments contain poorlyordered minerals, such as allophane. Generally, allophane is formed from tephra at pH values between 5 and 7 (Parfitt 2009). Different types of allophane contain different amounts of Al. Al-rich allophane has a Si:Al ratio of 0.5, while Si-rich allophane has a Si:Al ratio of 1 (Parfitt 2009), potentially explaining the range observed in our contaminant fractions. Other strong evidence of such origin lies in the much higher reactivity (k) of this fraction in NaOH, compared to the other non-BSi contaminant (Fig. 5). Allophane and other poorly ordered minerals are known to have a high specific surface area, thus a higher dissolution rate can be expected (Van Cappellen and Qiu 1997), especially in a strong base solution.

Comparison between traditional BSi determination and the new approach

Dissolution curves for Si and Al obtained with our detailed time-step analysis in 0.1 M Na_2CO_3 show similar dissolution patterns and Si:Al ratios to those obtained by continuous analysis of extraction in 0.5 M NaOH (Fig. 6), confirming that dissolution patterns and dynamics are similar at lower base strength. It is also clear that 0.1 M Na_2CO_3 extracts significant amounts of Al (e.g. the samples at 80–81 and

272–273 cm), indicating that it dissolves non-BSi fractions. This is confirmed by direct comparison of $AlkExSi_{Na_2CO_3}$and $AlkExSi_{NaOH}$ (Fig. 7), where the BSi content calculated from $AlkExSi_{NaOH}$ is always below or equal to the total AlkExSi extracted in Na_2CO_3 (Fig. 8). Microscopic observation of the residue left after extraction in 0.1 M Na_2CO_3 revealed no trace of diatoms in any of the 10 samples, confirming complete dissolution of the biogenic phase. In the majority of our 10 paired analyses, 0.1 M Na_2CO_3 also extracted the non-BSi fraction with Si:Al ratio<1, consistent with the notion that this fraction has a higher reactivity and will dissolve easily in an alkaline solution. At the same time, Na_2CO_3 seems to extract only a small part of the volcanic glass, as evidenced by the pure tephra sample (248–249 cm). In this case, the AlkExSi extracted in 0.1 M Na_2CO_3 is only 37 % of that extracted in 0.5 M NaOH.

Relationship between BSi and organic matter in lake sediments

The total biogenic component of sediments deposited in soft-water (non-carbonate) lakes is often considered to be the sum of organic matter (OM) and biogenic silica (Bradbury et al. 2004). Since diatom frustules contain both silica and organic carbon (OC) (Barker et al. 2013), a positive relationship between the concentrations of OM and BSi can be expected in sediments of lakes where diatoms constitute an important part of the algal flora.

Table 1 Parameters resulting from fitting Eq. 3 to raw Si and Al dissolution data from the continuous extraction. AlkExSi (in mg g^{-1}) is the concentration extracted in NaOH

Fraction:		BSi - AlkExSi				non-BSi - AlkExSi						Minerals					
Dissolution Pattern:		Sigmoidal Pattern				First Order			First Order			First Order			Linear		Total AlkExSi (mg g^{-1})
Sample depth (cm)	Age (years BP)	$AlkExSi_1$ (mg g^{-1})	No	k_1 (min^{-1})	$Si:Al_1$	$AlkExSi_2$ (mg g^{-1})	k_2 (min^{-1})	$Si:Al_2$	$AlkExSi_3$ (mg g^{-1})	k_3 (min^{-1})	$Si:Al_3$	$AlkExSi_4$ (mg g^{-1})	k_4 (min^{-1})	$Si:Al_4$	b (mg $g^{-1}min^{-1}$)	$Si:Al_{min}$	
24.5	64	19.33	2.13	0.63	$8.0x10^4$	-	-	-	15.53	0.52	0.42	-	-	-	0.29	0.99	34.86
32.5	188	15.28	0.33	0.91	860	30.03	0.27	160	-	-	-	-	-	-	0.23	1.36	45.31
40.5	389	31.46	3.97	0.68	$9.2 x10^4$	-	-	-	14.12	0.55	0.40	-	-	-	0.36	1.82	45.58
48.5	659	17.59	0.52	0.88	$1.5 x10^3$	31.16	0.24	390	-	-	-	-	-	-	0.22	1.26	48.75
56.5	987	26.16	3.39	0.64	$2.1 x10^3$	-	-	-	12.45	0.53	0.38	-	-	-	0.21	1.23	38.60
64.5	1365	21.16	1.31	0.78	$1.0 x10^9$	29.90	0.24	74	-	-	-	-	-	-	0.11	0.60	51.06
72.5	1784	19.44	1.98	0.62	$2.0 x10^5$	-	-	-	18.42	0.56	0.49	-	-	-	0.27	1.26	37.87
80.5	2233	32.39	4.07	0.61	$3.0 x10^5$	-	-	-	15.38	0.54	0.44	-	-	-	0.35	1.69	47.77
88.5	2705	30.03	2.85	0.66	$2.8 x10^4$	-	-	-	14.35	0.58	0.44	-	-	-	0.32	1.36	44.37
96.5	3190	21.25	0.92	0.71	$4.0 x10^5$	-	-	-	18.71	0.50	0.50	-	-	-	0.32	1.95	39.95
104.5	3679	21.36	0.58	0.84	$5.0 x10^4$	-	-	-	15.17	0.56	0.49	-	-	-	0.69	2.70	36.53
112.5	4162	13.37	0.12	1.00	$1.9 x10^3$	31.48	0.15	556	6.46	0.47	0.20	-	-	-	0.04	0.24	51.31
120.5	4630	20.95	0.39	0.80	$2.4 x10^3$	30.56	0.25	665	-	-	-	-	-	-	0.24	1.38	51.51
128.5	5075	25.69	1.03	0.79	$1.0 x10^4$	25.13	0.26	176	-	-	-	-	-	-	0.30	1.48	50.82
136.5	5486	36.05	1.97	0.60	$2.5 x10^3$	-	-	-	26.51	0.50	0.48	-	-	-	0.46	3.48	62.57
144.5	5873	79.57	9.36	0.60	$2.0 x10^8$	-	-	-	18.70	0.44	0.75	-	-	-	0.18	1.49	98.28
152.5	6239	58.44	4.77	0.64	$3.5 x10^3$	37.61	0.20	102	-	-	-	-	-	-	0.21	0.98	96.05
160.5	6497	14.31	0.09	0.91	$2.5 x10^3$	27.27	0.19	166	1.72	0.47	0.05	-	-	-	0.20	0.92	43.30
168.5	6636	27.39	0.70	0.73	$1.7 x10^3$	43.76	0.19	255	-	-	-	-	-	-	0.11	0.83	71.14

Table 1 continued

Fraction:		BSi - AlkExSi				non-BSi - AlkExSi						Minerals					
Dissolution Pattern:		Sigmoidal Pattern				First Order			First Order			First Order			Linear		Total AlkExSi (mg g^{-1})
Sample depth (cm)	Age (years BP)	$AlkExSi_1$ (mg g^{-1})	No	k_1 (min^{-1})	$Si:Al_1$	$AlkExSi_2$ (mg g^{-1})	k_2 (min^{-1})	$Si:Al_2$	$AlkExSi_3$ (mg g^{-1})	k_3 (min^{-1})	$Si:Al_3$	$AlkExSi_4$ (mg g^{-1})	k_4 (min^{-1})	$Si:Al_4$	b (mg $g^{-1}min^{-1}$)	$Si:Al_{min}$	
176.5	6925	36.61	2.76	0.61	2.0×10^6	-	-	-	15.60	0.48	0.57	-	-	-	0.29	1.97	52.21
184.5	7423	43.30	3.90	0.56	1.0×10^7	-	-	-	17.07	0.41	0.61	-	-	-	0.35	1.59	60.37
188.5	7733	15.72	0.18	0.84	294	30.71	0.20	11	-	-	-	-	-	-	0.32	1.55	46.43
192.5	8075	17.70	1.24	0.59	7.0×10^5	-	-	-	19.00	0.50	0.57	-	-	-	0.30	2.42	36.69
196.5	8447	24.11	2.31	0.57	1.0×10^6	-	-	-	17.27	0.47	0.57	-	-	-	0.38	1.77	41.38
200.5	8867	35.46	4.83	0.51	9.7×10^3	-	-	-	18.66	0.48	0.61	-	-	-	0.32	1.82	54.12
204.5	9356	29.59	2.60	0.58	1.3×10^6	-	-	-	15.96	0.43	0.58	-	-	-	0.31	1.65	45.55
208.5	9930	24.63	0.32	0.80	11	67.48	0.15	14	-	-	-	-	-	-	0.24	0.68	92.11
212.5	10556	16.19	1.12	0.64	6.0×10^6	-	-	-	22.59	0.43	0.84	-	-	-	0.39	0.98	38.78
216.5	11172	9.78	0.28	0.71	1.2×10^3	-	-	-	7.59	0.38	0.37	26.30	0.13	4.92	0.17	0.72	17.37
220.5	11720	9.44	0.42	0.51	201	-	-	-	26.71	0.39	0.72	-	-	-	0.41	1.08	36.15
224.5	12163	10.11	0.27	0.57	9.0×10^4	-	-	-	18.80	0.40	0.62	46.86	0.10	2.69	0.18	0.72	28.91
231.5	12744	6.56	0.13	0.50	3	32.00	0.26	31	-	-	-	-	-	-	0.42	1.22	38.57
240.5	13376	8.26	0.11	0.83	1.0×10^3	52.91	0.17	50	-	-	-	-	-	-	0.35	0.84	61.17
248.5		-	-	-		19.85	0.54	102	-	-	-	26.26	0.09	6.27	0.74	1.93	19.85
256.5	14113	7.42	0.06	0.73	8.1×10^3	-	-	-	36.77	0.73	1.18	34.46	0.03	1.03	0.01	10000	44.19
263.5	14604	12.16	0.33	0.52	3.0×10^5	-	-	-	43.68	0.52	1.12	-	-	-	0.43	1.18	55.84
264.5	14674	12.27	1.02	0.41	2.0×10^5	-	-	-	37.98	0.41	0.99	-	-	-	0.45	0.91	50.24

Table 1 continued

Fraction:		BSi - AlkExSi				non-BSi - AlkExSi						Minerals					
Dissolution Pattern:		Sigmoidal Pattern				First Order			First Order			First Order			Linear		Total AlkExSi (mg g^{-1})
Sample depth (cm)	Age (years BP)	$AlkExSi_1$ (mg g^{-1})	No	k_1 (min^{-1})	$Si:Al_1$	$AlkExSi_2$ (mg g^{-1})	k_2 (min^{-1})	$Si:Al_2$	$AlkExSi_3$ (mg g^{-1})	k_3 (min^{-1})	$Si:Al_3$	$AlkExSi_4$ (mg g^{-1})	k_4 (min^{-1})	$Si:Al_4$	b (mg $g^{-1}min^{-1}$)	$Si:Al_{min}$	
272.5	15235	12.60	0.86	0.38	6	-	-	-	42.25	0.38	1.07	-	-	-	0.40	1.09	54.85
280.5	15797	11.96	0.56	0.42	50	-	-	-	42.87	0.42	1.01	-	-	-	0.47	1.06	54.82
288.5	16358	12.70	0.82	0.43	7.0×10^5	-	-	-	40.93	0.43	1.04	-	-	-	0.42	1.04	53.63
296.5	16919	11.81	0.68	0.39	1.0×10^6	-	-	-	49.28	0.39	1.14	-	-	-	0.36	0.87	61.10
304.5	17480	10.29	0.13	0.52	508	53.02	0.24	40	-	-	-	-	-	-	0.42	1.53	63.31
320.5	18498	13.35	0.21	0.48	12	60.13	0.19	999	-	-	-	-	-	-	0.30	0.80	73.47

In the present study, the relationship is significant (r = 0.671; p =<0.01) only when we correlate %OM with %BSi after exclusion of contaminating non-biogenic fractions (Fig. 9). If the total AlkExSi concentration is used (as is traditionally done in the DeMaster method), no correlation is observed (r = -0.019). This result confirms our hypothesis: the traditional method extracts more fractions than just BSi, compromising the expected link between diatoms and organic matter. This result shows that the methodology proposed in this study is capable of correctly isolating the true biogenic contribution to AlkExSi.

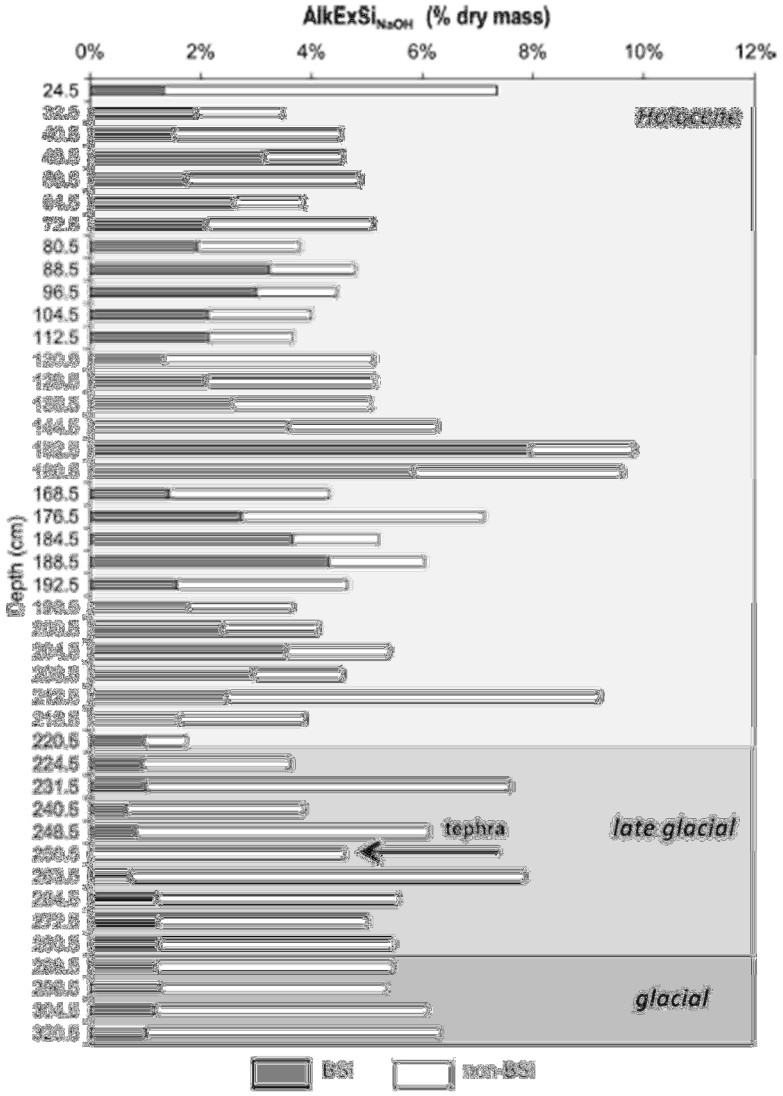

Fig. 4 Stacked BSi and non-BSi fractions (% of total dry mass) in 43 Lake Rutundu sediment samples spanning the last 21,000 years, determined using continuous analysis of Si and Al extracted in 0.5 M NaOH

Several past studies from sites worldwide have attempted to account for absent or strange correlations between BSi and OC in lake sediments (Felton et al. 2007; Lü et al. 2010; Govil et al. 2011; Theissen et al. 2012; Chawchai et al. 2013; Liu et al. 2014). Some of these results may reflect the fact that sedimentaryOMin lacustrine environments can also derive from algae other than diatoms, or from terrestrial plants or bacteria (Meyers and Ishiwatari 1993; Meyers and Teranes 2001). Conversely, a significant part of the BSi measured in lake sediments may be derived from plant phytoliths contained in eroding terrestrial soils (Saccone et al. 2007). In other cases, changing redox conditions at the sediment–water interface may alterOMpreservation while leaving diatoms unaffected (Kristensen and Holmer 2001). However, the sheer contrast in level of correlation between BSi and OM content observed here strongly suggests that also the methodology used to estimate BSi may be partly responsible for these discrepancies. We hypothesize that the magnitude of discrepancy may be a function of interference from nonbiogenic Si in volcanic materials, possibly enhanced by high clastic dilution of the OM and BSi.

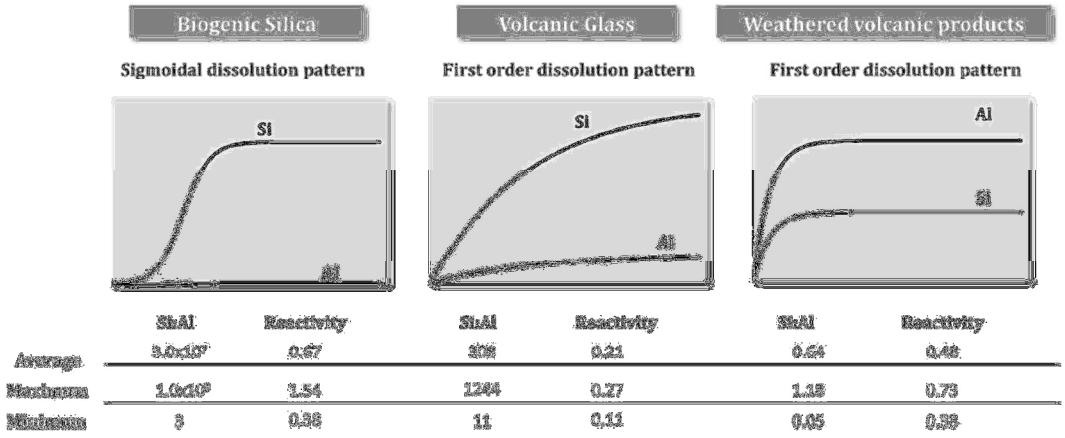

	Si:Al	Reactivity	Si:Al	Reactivity	Si:Al	Reactivity
Average	3.0x10⁵	0.67	208	0.21	0.64	0.48
Maximum	1.0x10⁶	1.54	1244	0.27	1.18	0.73
Minimum	3	0.36	11	0.11	0.05	0.38

Fig. 5 Schematic dissolution patterns of the three main fractions identified in the AlkExSi pool, with minimum, maximum and average Si:Al ratios and reactivity (min^{-1}) values

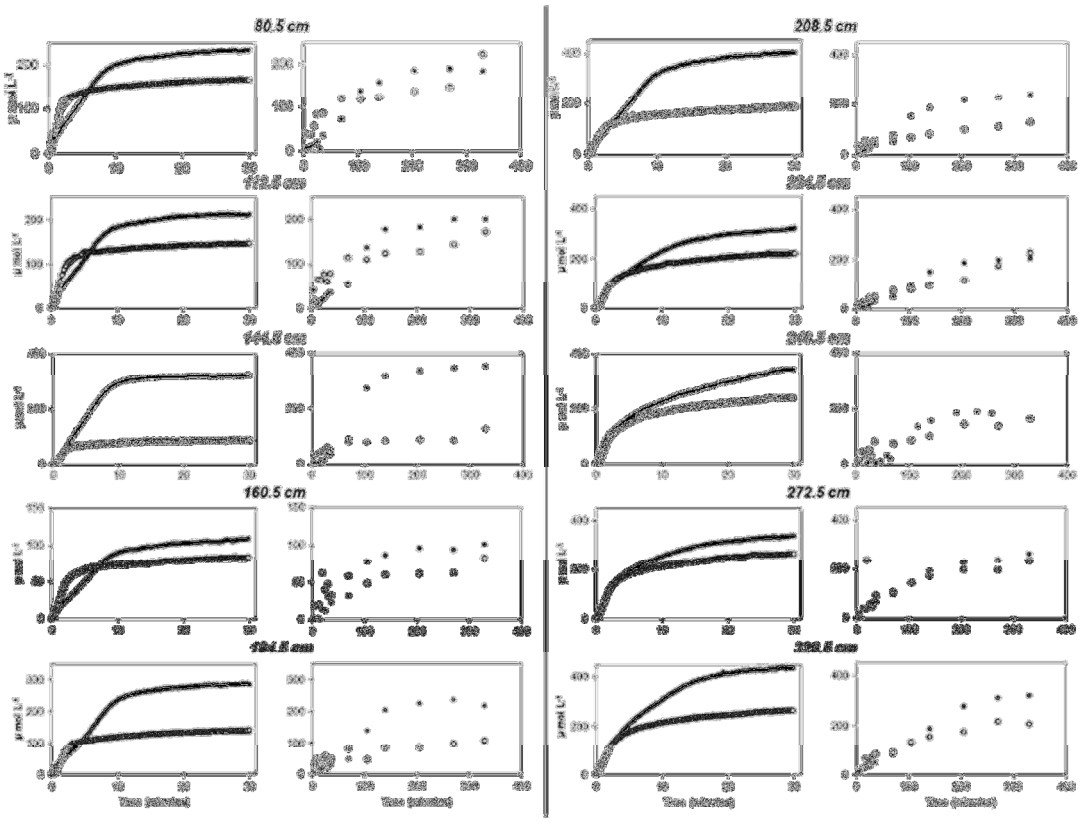

Fig. 6 Dissolution curves of Si (black circles) and Al (white circles; both in lmol L^{-1}) obtained with continuous analysis of AlkExSi extracted in 0.5 M NaOH (left panels of each column) and with a detailed time-step analysis of AlkExSi extracted in 0.1 M Na_2CO_3 (right panels of each column). The full black lines represent the best-fitting models for the continuous data

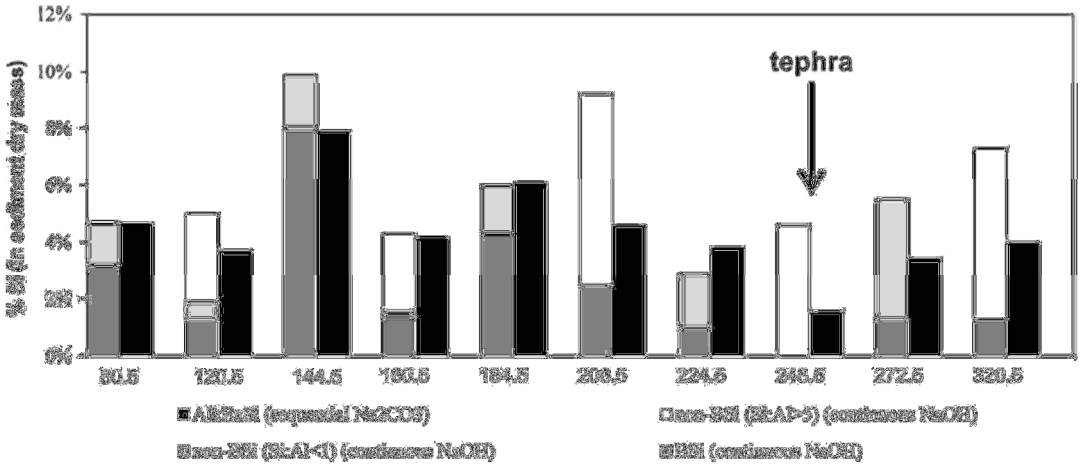

Fig. 7 Paired analysis of BSi and non-BSi fractions (% of total dry mass) in 10 representative Lake Rutundu samples, using either continuous analysis of AlkExSi extracted in 0.5 MNaOH (taking into account the separation) or time-step analysis of AlkExSi extracted in 0.1 M Na_2CO_3 (after mineral correction)

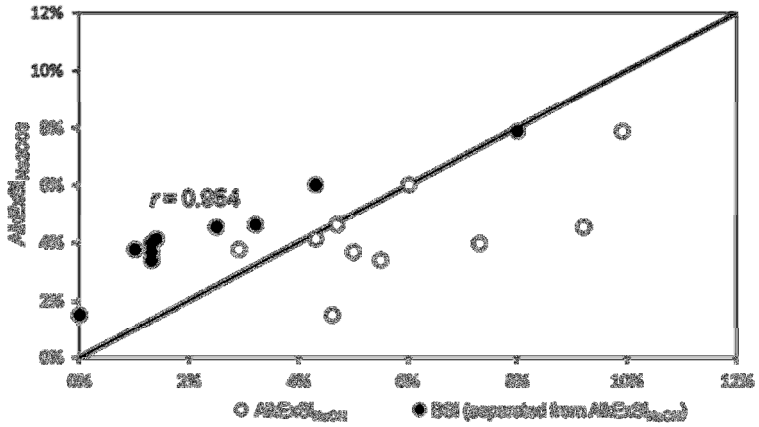

Fig. 8 Correspondence between $AlkExSi_{Na2CO3}$ derived from time-step analysis, and total $AlkExSi_{NaOH}$ and BSi (separated from the $AlkExSi_{NaOH}$), both derived from continuous analysis

Implications

Continuous analysis of Si and Al extracted from Lake Rutundu sediments successfully proved our hypothesis that other sedimentary Si fractions dissolved in alkaline environments besides BSi can result in significant overestimation of true BSi (diatom Si), and may bias the temporal signal in BSi variation (and thus diatom productivity) measured throughout a lakesediment sequence. The idea that NaOH extracts Si fractions besides BSi has been explored before in many different ecosystems (Kamatani and Oku, 2000; Koning et al. 2002; Saccone et al. 2007), and is one reason why Na_2CO_3 is more widely used to assess sedimentary BSi content. However, our experiment demonstrates that also Na_2CO_3 dissolves non-biogenic Si, and may likewise overestimate true diatom concentrations in lake sediments. The strong correlation ($r = 0.954$; $p =<0.01$) observed here between $AlkExSi_{Na2CO3}$ and corrected BSi extracted in NaOH (Fig. 8) supports the idea that a uniform correction can be made for the entire Lake Rutundu sequence, but the magnitude of this correction is most likely specific to the catchment geology of individual lakes. The mathematical tool presented here is capable of differentiating between biogenic Si, amorphous volcanic glass, and a second contaminant likely consisting of poorly-ordered mineral silicates such as allophane. The fact that volcanic glass may be an important source of contamination in BSi measurements has been noted before (Clymans et al. 2014; Cornelis et al. 2014). In reference to Lake Rutundu, Street-Perrott et al. (2008) cited specifically this reason as their motivation for estimating diatom productivity through direct counting of diatom abundance and biovolume calculations (Barker et al. 2000). We provide an alkaline-extraction approach that gets around this problem. Still, variability of tephra and its weathering products both in structure and composition (Ninkovich 1979; Parfitt and Furkert 1980; Lowe 1988; Pollard et al. 2003) argues against a simple extrapolation of our equations to other lakes subject to volcanic interference, given that measurement of the isolated contaminants is

crucial to calibrate the equations. With this in mind, we hypothesize that our general method is also suitable for other types of aquatic systems, such as turbid reservoirs, where abundant fine-grained clastic mineral input rather than equations. With this in mind, we hypothesize that our general method is also suitable for other types of aquatic systems, such as turbid reservoirs, where abundant fine-grained clastic mineral input rather than volcanic materials may be an important source of nonbiogenic AlkExSi. In terms of laboratory procedure, we emphasize that our approach to BSi determination is complex and more time-consuming than the traditional DeMaster method. In continuous analysis on an auto-analyzer, samples are processed individually rather than simultaneously as a batch, and each requires ca. 30 min for extraction plus time for cleaning, instrument re-calibration and reagent preparation. Additionally, the mathematical calculations are more advanced and require substantial attention. We therefore recommend careful evaluation of the necessity of using the continuous extraction, by first examining catchment geology and other possible sources of BSi contamination. Volcanic activity in East Africa, western North and South America and in large parts of Asia is likely a significant source of readily dissolvable volcanic material to lakes. In non-volcanic regions, e.g. much of the northern high-latitude regions of Eurasia, North America and Greenland, its contaminating effect may be relatively minor. However, soil erosion, runoff events and riverine input can still transport reactive mineral and pedogenic materials that dissolve fast and contribute to total AlkExSi in lakes worldwide. Consideration of the lake's setting, including its geology and landscape integration (area, slope, vegetation cover) should provide indications about the possible sources and significance of potential BSi contamination. In situations where non-biogenic contamination may be suspected, we recommend using the continuous analysis of at least a representative subset of the samples used to construct a sedimentary BSi profile, so as to evaluate the impact of any contaminants both on absolute %BSi values and their trends through time. When paleoenvironmental reconstructions require BSi time series at high temporal resolution, continuous analysis and subsequent modelling of the constituent fractions on this subset of samples can be used to determine a site-specific correction factor which allows to convert AlkExSi values into proper estimations of true biogenic Si. In the case of Lake Rutundu, separation of BSi from non-biogenic fractions using the continuous analysis shows a general increase in BSi concentration from the glacial and late-glacial periods to the Holocene. Previous research on the sediment record of this lake (Street-Perrott et al. 2008) pointed to a different trend in the abundance of fossil diatoms, with total diatom biovolume being highest in the glacial period (see also Fig. 1b–d). While the chemical extraction technique used in our present study targets all Si of biogenic origin, Street-Perrott et al. (2008) directly counted diatoms on microscope preparations of the core samples, thus visually separating diatoms from other sources of BSi, such as plant phytoliths. Although a full paleoenvironmental analysis of the combined terrestrial and aquatic ecosystems on Mt.Kenya is beyond the scope of this paper, this implies that chemical extraction alone does not suffice to uniquely characterize long-term trends in diatom productivity in this system. For example, rapid Si cycling in the mesic but seasonally fire-prone alpine grassland occupying the Lake Rutundu area in the early Holocene period of enhanced monsoon rainfall and seasonality (Ficken et al. 2002; Street-Perrott et al.
2008) may have created a temporally enhanced influx of visually undiagnostic phytolith fragments to Lake Rutundu sediments. This observation highlights the fact that analytical methods should always follow closely a study's intentions and be interpreted accordingly (Barão et al. 2015). The methodology presented here allows separating BSi from non-biogenic (in this case volcanic) interference products, but for detailed paleoenvironmental assessment of trends in diatom productivity through time a combination of quantitative chemical methods and (at least qualitative) optical methods of lake-sediment investigation is necessary.

Acknowledgments L.B. thanks Special Research Funding from the University of Antwerp (BOF-UA and NOI) for a PhD fellowship. E.S. thanks FWO-Vlaanderen (Research Foundation Flanders) for postdoctoral research funding. The fieldwork in Mt. Kenya National Park was conducted under permits from Kenya's National Council for Science and Technology (NCST/ RCD/14/012/14) and National Environmental Monitoring Authority (NEMA AGR/7/2010), and exported for analysis under Material Transfer Agreement A11/TT/1040 between the Kenya Wildlife Service, the University of Nairobi, and Ghent University. We thank Tom van der Spiet and Anne Cools for laboratory assistance in developing the method, and two anonymous referees for constructive comments that improved the final manuscript.

References

Barão L, Clymans W, Vandevenne F, Meire P, Conley DJ, Struyf E (2014) Pedogenic and biogenic alkaline-extracted silicon distributions along a temperate land-use gradient. Eur J Soil Sci 65:693–705

Barão L, Vandevenne F, Clymans W, Frings P, Ragueneau O, Meire P, Conley DJ, Struyf E (2015) Alkaline-extractable silicon from land to ocean: a challenge for biogenic silicon determination. Limnol Oceanogr: Methods. doi:10.1002/ lom3.10028

Barker PA, Perrott RA, Ficken KJ, Swain DL (2000) Diatom palaeoproductivity in a high-altitude lake on Mt. Kenya: preliminary results from Lake Rutundu. Verhandlungen der internationale Vereinigung der Limnologie 27:1003–1007

Barker P, Hurrell ER, Leng MJ, Plessen B, Wolff C, Conley DJ, Keppens E, Milne I, Cumming BF, Laird KR, Kendrick CP, Wynn PM, Verschuren D (2013) Carbon cycling within an East African lake revealed by the carbon isotope composition of diatom silica: a 25-ka record from LakeChalla, Mt. Kilimanjaro. Quat Sci Rev 66:55–63

Battarbee RW, Jones VJ, Flower RJ, Cameron NG, Bennion H, Carvalho L, Juggins S (2001) Diatoms (JP Smol, HJB Birks, WM Last, RS Bradley, and K Alverson, Eds.). Dev Paleoenviron Res 3:155–202

Bradbury JP, Colman SM, Dean WE (2004) Limnological and climatic environments at upper Klamath Lake, Oregon during the past 45000 years. J Paleolimnol 31:167–188

Broecker WS (1994) Massive iceberg discharges as triggers for global climate change. Nature 372:421–424

Carey JC, Fulweiler RW (2012) Human activities directly alter watershed dissolved silica fluxes. Biogeochemistry 111: 125–138

Chawchai S, Chabangborn A, Kylander M, Lo¨wemark L, Mo¨rth C-M, Blaauw M, Klubseang W, Reimer PJ, Fritz SC, Wohlfarth B (2013) Lake Kumphawapi—an archive of Holocene palaeoenvironmental and palaeoclimatic changes in northeast Thailand. Quat Sci Rev 68:59–75

Clymans W, Lehtinen T, Gı´slado´ ttir G, Lair GJ, Barão L, Ragnarsdóttir KV, Struyf E, Conley DJ (2014) Si precipitation during weathering in different Icelandic Andosols. Proc Earth Planet Sci 10:260–265

Conley DJ (1988) Biogenic silica as an estimate of siliceous microfossil abundance in Great Lakes sediments. Biogeochemistry 6:161–179

Conley DJ (2002) Terrestrial ecosystems and the global biogeochemical silica cycle. Glob Biogeochem Cycles 16:1121

Conley DJ, Schelske CL (2001) Tracking environmental change using lake sediments: terrestrial, algal, and siliceous indicators. Dev Paleoenviron Res 3:281–293

Conley DJ, Stalnacke P, Pitkanen H, Wilander A (2000) The transport and retention of dissolved silicate by rivers in Sweden and Finland. Limnol Oceanogr 45:1850–1853

Cornelis JT, Delvaux B, Georg RB, Lucas Y, Ranger J, Opfergelt S (2011) Tracing the origin of dissolved silicon transferred from various soil-plant systems towards rivers: a review. Biogeosciences 8:89–112

Cornelis JT, Dumon M, Tolossa AR, Delvaux B, Deckers J, Van Ranst E (2014) The effect of pedological conditions on the sources and sinks of silicon in the Vertic Planosols in south-western Ethiopia. Catena 112:131–138

DeanWE(1974) Determination of carbonate and organic matter in calcareous sediments and sedimentary rocks by loss on ignition: comparison with other methods. J Sediment Petrol 44:242–248

DeMaster DJ (1981) The supply and accumulation of silica in the marine environment. Geochim Cosmochim Acta 45:1715–1732

Felton AA, Russell JM, Cohen AS, Baker ME, Chesley JT, Lezzar KE, McGlue MM, Pigati JS, Quade J, Curt Stager J, Tiercelin JJ (2007) Paleolimnological evidence for the onset and termination of glacial aridity from Lake Tanganyika, Tropical East Africa. Palaeogeogr Palaeoclimatol Palaeoecol 252:405–423

Ficken KJ, Wooller MJ, Swain D, Street-Perrott FA, Eglinton G (2002) Reconstruction of a subalpine grass-dominated ecosystem, Lake Rutundu, Mount Kenya: a novel multiproxy approach. Palaeogeogr Palaeoclimatol Palaeoecol 177:137–149

Finkelstein SA, Gajewski K (2007) A palaeolimnological record of diatom-community dynamics and late-Holocene climatic changes from Prescott Island, Nunavut, central Canadian Arctic. The Holocene 17:803–812

Frings PJ, Clymans W, Jeppesen E, Lauridsen TL, Struyf E, Conley DJ (2014) Lack of steady-state in the global biogeochemical Si cycle: emerging evidence from lake Si sequestration. Biogeochemistry 117:255–277

Govil P, Mazumder A, Tiwari A, Kumar S (2011) Holocene climate variability from Lake sediment core in Larsemann Hills, Antarctica. J Geol Soc India 78:30–35

Grasshoff K, Kremling K, Ehrhardt M (1983) Methods of seawater analysis. Wiley-Vch Verlag GmbH, Weinheim

Hartmann J, Jansen N, Du¨rr HH, Harashima A, Okubo K, Kempe S (2009) Predicting riverine dissolved silica fluxes to coastal zones from a hyperactive region and analysis of their first-order controls. Int J Earth Sci 99:207–230

Humborg C, Conley DJ, Rahm L, Wulff F, Cociasu A, Ittekkot V (2000) Silicon retention in river sasins: far-reaching effects on biogeochemistry and aquatic food webs in coastal marine environments. Ambio 29:45–50

Hydes DJ, Liss PS (1976) Fluorimetric method for the determination of low concentrations of dissolved aluminium in natural waters. The Analyst 101:922–931

Johnson TC, Barry SL, Chan Y, Wilkinson P (2001) Decadal record of climate variability spanning the past 700 yr in the Southern Tropics of East Africa. Geology 29:83–86

Johnson TC, Brown ET, McManus J, Barry S, Barker P, Gasse F (2002) A high-resolution paleoclimate record spanning the past 25,000 years in southern East Africa. Science 296:113–132

Kamatani A, Oku O (2000) Measuring biogenic silica in marine sediments. Mar Chem 68:219–229

Koning E, van Iperen JM, van Raaphorst W, Helder W, Brummer G-JA, van Weering TCE (2001) Selective preservation of upwelling-indicating diatoms in sediments off Somalia, NW Indian Ocean. Deep Sea Res Part I 48:2473–2495

Koning E, Epping E, van Raaphorst W (2002) Determining biogenic silica in marine samples by tracking silicate and aluminium concentrations in alkaline leaching solutions. Aquat Geochem 8:37–67

Kristensen E, Holmer M (2001) Decomposition of plant materials in decomposition of plant materials in marine sediment exposed to different electron acceptors (O_2, NO_3^-,SO_4^{2-})with emphasis on substrate origin, degradation kinetics, and the role of bioturbation. Geochim Cosmochim Acta 65:419–433

Laruelle GG, Roubeix V, Sferratore A, Brodherr B, Ciuffa D, Conley DJ, Du¨ rr HH, Garnier J, Lancelot C, Le Thi Phuong Q, Meunier J-D, Meybeck M, Michalopoulos P, Moriceau B, Nı´ Longphuirt S, Loucaides S, Papush L, Presti M, Ragueneau O, Regnier P, Saccone L, Slomp CP, Spiteri C, Van Cappellen P (2009) Anthropogenic perturbations of the silicon cycle at the global scale: key role of the landocean transition. Glob Biogeochem Cycles 23:1–17

Leng MJ, Barker PA (2006) A review of the oxygen isotope composition of lacustrine diatom silica for palaeoclimate reconstruction. Earth Sci Rev 75:5–27

Liu B, Xu H, Lan J, Sheng E, Che S, Zhou X (2014) Biogenic silica contents of Lake Qinghai sediments and its environmental significance. Front Earth Sci 8:573–581

Lowe DJ (1988) Stratigraphy, age, composition, and correlation of late Quaternary tephras interbedded with organic sediments in Waikato lakes, North Island, New Zealand. NZ J Geol Geophys 31:125–165

Lü C-W, He J, Liang Y, Mao H-F, Liu H-L, Wang F-J (2010) Temporal and spatial distribution of biogenic silica and its significance in the Wuliangsuhai Lake and Daihai Lake. Acta Ecol Sin 30:100–105

Meyers PA, Ishiwatari R (1993) Lacustrine organic geochemistrym— an overview of indicators of organic matter sources and diagenesis in lake sediments. Org Geochem 20:867–900

Meyers PA, Teranes JL (2001) Sediment organic matter (WM Last and JP Smol, Eds.). Dev Paleoenviron Res 2:239–269 Mortlock RA, Froelich PN (1989) Instruments and methods—a simple method for the rapid determination of biogenic opal in pelagic marine sediments. Deep Sea Res Part A. Oceanogr Res Papers 36:1415–1426 Ninkovich D (1979) Distribution, age and chemical composition of tephra layers in deep-sea sediments off western Indonesia. J Volcanol Geoth Res 5:67–68

Parfitt RL (2009) Allophane and imogolite: role in soil biogeochemical processes. Clay Miner 44:135–155

Parfitt RL, Furkert RJ (1980) Identification and structure of two types of allophane from volcanic ash soils and tephra. Clays Clay Miner 28:328–334

Pollard AM, Blockley SPE, Ward KR (2003) Chemical alteration of tephra in the depositional environment: theoretical stability modelling. J Quat Sci 18:385–394

Ragueneau O, Treguer P, Leynaert A, Anderson RF, Brzezinski MA, Demaster DJ, Dugdale RC, Dymond J, Fischer G, Franc R, Heinze C, Nelson DM, Queguiner B (2000) A review of the Si cycle in the modern ocean: recent progress and missing gaps in the application of biogenic opal as a paleoproductivity proxy. Glob Planet Chang 26:317–365

Ragueneau O, Savoye N, Del Amo Y, Cotten J, Tardiveau B, Leynaert A (2005) A new method for the measurement of biogenic silica in suspended matter of coastal waters: using Si:Al ratios to correct for the mineral interference. Cont Shelf Res 25:697–710

Ragueneau O, Schultes S, Bidle K, Claquin P, Moriceau B (2006) Si and C interactions in the world ocean: importance of ecological processes and implications for the role of diatoms in the biological pump. Glob Biogeochem Cycles 20:1–15

Raimonet M, Ragueneau O, Jacques V, Corvaisier R, Moriceau B, Khripounoff A, Pozzato L, Rabouille C (2014) Rapid transport and high accumulation of amorphous silica in the Congo deep-sea fan: a preliminary budget. J Mar Syst 141:71–79

Ren H, Brunelle BG, Sigman DM, Robinson RS (2013) Diagenetic aluminum uptake into diatom frustules and the preservation of diatom-bound organic nitrogen. Mar Chem 155:92–101

Saccone L, Conley DJ, Koning E, Sauer D, Sommer M, Kaczorek D, Blecker SW, Kelly EF (2007) Assessing the extraction and quantification of amorphous silica in soils of forest and grassland ecosystems. Eur J Soil Sci 58:1446–1459

Schelske CL, Stoermer EF, Conley DJ, Robbins JA, Glover RM (1983) Early eutrophication in the lower Great Lakes: new evidence from biogenic silica sediments. Science 222:321–322

Smol JP, Cumming BF (2000) Review tracking long-term changes in climate using algal indicators in lake sediments. J Phycol 36:986–1011

Stoermer EF, Smol JP (1999) The diatoms: applications for the environmental and earth sciences. Cambridge University Press, Cambridge

Street-perrott FA, Barker PA (2008) Biogenic silica: a neglected component of the coupled global continental biogeochemical cycles of carbon and silicon. Earth Surf Proc Land 1457:1436–1457

Street-Perrott FA, Ficken KJ, Huang Y, Eglinton G (2004) Late Quaternary changes in carbon cycling on Mt. Kenya, East Africa: an overview of the d13C record in lacustrine organic matter. Quat Sci Rev 23:861–879

Street-perrott FA, Barker PA, Swain DL, Ficken KJ, Wooller MJ, Olago DO, Huang Y (2007) Late Quaternary changes in ecosystems and carbon cycling on Mt. Kenya, East Africa: a landscape-ecological perspective based on multiproxy lake-sediment influxes. Quat Sci 26:1838–1860

Street-Perrott FA, Barker PA, Leng MJ, Sloane HJ, Wooller MJ, Ficken KJ, Swain DL (2008) Towards an understanding of late Quaternary variations in the continental biogeochemical cycle of silicon : multi-isotope and sediment-flux data for Lake Rutundu, Mt Kenya, East Africa, since 38 ka BP. J Quat Sci 23:375–387

Struyf E, Conley DJ (2012) Emerging understanding of the ecosystem silica filter. Biogeochemistry 107:9–18

Struyf E, Smis A, Van Damme S, Garnier J, Govers G, Van Wesemael B, Conley DJ, Batelaan O, Frot E, Clymans W, Vandevenne F, Lancelot C, Goos P, Meire P (2010) Historical land use change has lowered terrestrial silica mobilization. Nat Commun 1:129

Theissen KM, Hobbs WO, Hobbs JMR, Zimmer KD, Domine LM, Cotner JB, Sugita S (2012) The altered ecology of Lake Christina: a record of regime shifts, land-use change, and management from a temperate shallow lake. Sci Total Environ 433:336–346

Tréguer PJ, De La Rocha CL (2013) The world ocean silica cycle. Annu Rev Mar Sci 5:477–501

Van Bennekom AJ, Janse JHF, van der Gaast SJ, van Iperen JM, Pieters J (1989) Aluminium rich opal: an intermediate in the preservation of biogenic silica in the Zaire (Congo) deep-sea fan. Deep Sea Res Part A. Oceanogr Res Papers 36:173–190

Van Cappellen P, Qiu L (1997) Biogenic silica dissolution in sediments of the Southern Ocean. I. Solubility. Deep Sea Res Part II: Trop Stud Oceanogr 44:1109–1128

Verschuren D, Johnson TC, Kling HJ, Edgington DN, Leavitt PR, Brown ET, Talbot MR, Hecky RE (2002) History and timing of human impact on Lake Victoria, East Africa. Proc R Soc B: Biol Sci 269:289–294

Wooller MJ, Swain DL, Ficken KJ, Agnew ADQ, Street-Perrott FA, Eglinton G (2003) Late Quaternary vegetation changes around Lake Rutundu, Mount Kenya, East Africa: evidence from grass cuticles, pollen and stable carbon isotopes. J Quat Sci 18:3–15